






The Orbital Angular Momentum of Azimuthal Spin-Waves

T. Valet ^{1,*} K. Yamamoto ² B. Pigeau ³ G. de Loubens ⁴ and O. Klein ^{1,†}

¹ *Universit Grenoble Alpes, CEA, CNRS, Grenoble INP, Spintec, 38054 Grenoble, France*

² *Advanced Science Research Center, Japan Atomic Energy Agency, Tokai, Ibaraki 319-1195, Japan*

³ *Universit Grenoble Alpes, CNRS, Grenoble INP, Institut Nel, Grenoble, France*

⁴ *SPEC, CEA, CNRS, Universit Paris-Saclay, 91191 Gif-sur-Yvette, France*

(Dated: March 12, 2025)

In the context of a growing interdisciplinary interest in the angular momentum of wave fields, the spin-wave case has yet to be fully explored, with the extensively studied notion of spin transport being only part of the broader picture. Here we report experimental evidence for non-zero magnon orbital angular momentum inside magnetic disk, by resolving the frequency splitting between magnon modes with counter-rotating wavefronts and thereby avoiding formation of azimuthal standing waves. This requires an unambiguous formulation of spin and orbital angular momenta for spin waves, which we provide in full generality taking advantage of a systematic application of quantum field theory techniques as detailed in an associated article [1]. The results unequivocally establish magnetic dipole-dipole interactions as a magnetic-field controllable spin-orbit interaction for magnons. Our findings open a new research direction, leveraging the spectroscopic readability of angular momentum for azimuthal spin waves and other related systems.

There has been an increasing realization in recent decades of the fundamental importance of the angular momentum (AM) carried by wave fields [2, 3], which can be separated into spin (SAM) and orbital (OAM) components in certain cases. The latter is a universal feature of waves in uniform continuum media represented by helical or rotational wavefronts, and can potentially encode a large amount of information for mode multiplexed communication channels or multi-level registers of quantum states. Theoretical and experimental investigations of wave AM are already well developed for electromagnetic waves [4–6], plasma waves [7], fluid waves [8, 9] or elastic waves [10]. Acknowledging wave AM in solid state media should be termed pseudo AM [11, 12], we omit the prefix following the common practice of the magnetism community. In recent years, experiments have found AM transfer between spin-waves (SWs) and optical vortices [13–18], or elastic waves [19–24]. All of these works, however, appear to have focused on SAM of SWs, leaving their OAM counterpart experimentally unexplored, which may also be placed in the context of the general difficulty in directly observing wave OAM [25]. In magnetic vortices, it took a sophisticated Kerr or Brillouin light scattering (BLS) microscopy to spatially resolve the azimuthal wavefronts [26–29]. It remains unclear, however, whether they detected rotating wavefronts carrying nonzero OAM or merely a standing wave pattern without definite OAM despite dedicated theoretical studies [30–33].

In this Letter, we report on a spectroscopic measurement of SW eigenstates with nonvanishing OAM in a normally magnetized disk, an unambiguous signature of rotating wavefronts. This leverages on the broken time-reversal symmetry of magnetic excitations for which there is no reason for the modes with counter-rotating wavefronts to be degenerate. The assignment of OAM to spectral peaks, however, requires its unambiguous defi-

inition for linear SW dynamics. While a handful of theoretical works discuss AM of magnetization dynamics, none serves our purposes as they either specify certain geometries [16, 17, 34–37] or do not discuss azimuthal SW eigenstates [12, 38–41]. We shall also mention recent theories of OAM [42, 43] and spin-orbit interaction (SOI) [44] across the magnon Brillouin zone, which are distinct topics from long wavelength SWs in mesoscopic ferromagnets. As a prerequisite to the spectroscopic detection of AM eigenstates, therefore, we developed a general formulation of magnon AM that clarifies its relation to azimuthal SW eigenstates in any axisymmetric geometry, whose details are exposed in a separate article [1]. Here, we merely assemble the essential results and use them to interpret the experimental spectrum, although the theory is applicable to a much wider class of problems. Agreement with the experiment is quantitative, and establishes a spectroscopic measurement of OAM. Our findings lay a foundation for reading OAM states not only for SWs but also for phonons or photons that can hybridize with SWs, and thereby open a new research direction in the study of general wave AM.

Figure 1 shows the measured SW spectra near the saturation field, H_{sat} . The spectroscopy is conducted by a magnetic resonance force microscope (MRFM) [45], an instrument that probes the variation of the magnetization along the local equilibrium axis. This enables the detection of modes with nonuniform spatial profiles, which are difficult to characterize with conventional probes. The sample is a Yttrium Iron Garnet (YIG) microdisk, which has been patterned by Ar etching from a thin film grown by liquid phase epitaxy, with a diameter of $1\ \mu\text{m}$ and a thickness of 55 nm determined from the splitting between exchange SW modes observed by BLS. Subsequently, a radio-frequency antenna is deposited on its surface with a slight misalignment in the lateral posi-

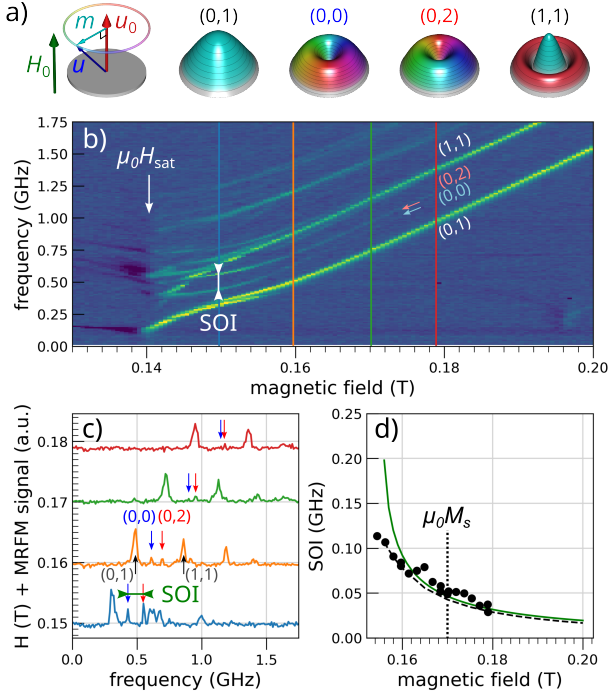


FIG. 1. a) Graphical representation of the precession pattern of $\mathbf{m}(\mathbf{x})$ for SW modes labeled (n_R, n_J) . b) MRFM spectrum as a function of normal magnetic field on a YIG disk. c) Line cuts at field values indicated by vertical lines of respective colors in b). The split between the (0, 2) and (0, 0) peaks defines the SOI. d) Magnetic field dependence of the SOI. The dots are the experimental points, while the solid and dashed lines are theoretical predictions, respectively assuming perfect alignment and a misalignment of 0.7° between the magnetic field and the normal of the disk.

tion, resulting in a gradient of the emitted microwave magnetic field along the diameter. As will be demonstrated, this gradient is sufficient to excite nonvanishing OAM SW modes. The apparatus is situated between the poles of an electromagnet that produces a large magnetic field, H_0 , aligned within $\pm 0.5^\circ$ of the disk normal. Figure 1b) is a density plot of the variation of the MRFM signal as a function of H_0 and the excitation frequency, $\omega/(2\pi)$. The spectral peaks are labeled by radial index $n_R \in \mathbb{Z}^+$ and azimuthal index $n_J \in \mathbb{Z}$, to be discussed in detail shortly. In this plot, the most intense signals arise from the Kittel mode $(n_R, n_J) = (0, 1)$, and its first radial harmonic (1, 1). Expected precession patterns of their dynamical magnetization $\mathbf{m}(\mathbf{x})$ are sketched in Fig. 1a) where the height indicates the amplitude and the color the azimuthal orientation (cf. colorwheel in Fig. 2). Because of their spatially uniform precession, these are naturally the modes coupled strongest to the antenna. By linearly fitting the variation of the (0, 1) mode frequency with the external magnetic field between 0.3 and 1 T, we determine the values of the gyromagnetic ratio $|\gamma| = 1.76 \times 10^{11} \text{ rad} \cdot \text{sec}^{-1} \cdot \text{T}^{-1}$ and saturation

magnetization $\mu_0 M_s = 0.17 \text{ T}$ where μ_0 is the vacuum permeability. Between these landmark eigenstates, we also observe two additional small peaks which can be uniquely assigned to the modes (0, 0) and (0, 2). No other modes are expected in this frequency range given our disk dimensions. These two eigenstates correspond to SW modes with counter-rotating wavefronts, as illustrated in Fig. 1a). While they are almost degenerate above 0.18 T, they increasingly split in frequency as H_0 approaches H_{sat} from above. We will establish below that this is due to the dynamical dipolar interaction (DDI), whose influence increases with decreasing H_0 . It introduces an ellipticity in the spin precession of the homogeneously magnetized disk and acts as a SOI for SW. The field-controllable SOI can be made much larger than the linewidth by tuning H_0 closer to H_{sat} , making the split readily observable.

To substantiate the claims made in the previous paragraph, we set up a theoretical model, relate SW eigenstates to OAM, and compute their spectrum. Consider a ferromagnet occupying a region Ω , whose magnetization is given by $\mathbf{M}(\mathbf{x}, t) = M_s \mathbf{u}(\mathbf{x}, t)$, with $\mathbf{u}(\mathbf{x}, t)$ a time dependent unit vector field (Fig. 1a)). We assume the existence of a textured equilibrium, $\mathbf{u}_0(\mathbf{x})$, and define the dimensionless SW field $\mathbf{m} = \mathbf{u} - \mathbf{u}_0$. The linear dynamics of \mathbf{m} is determined by minimizing the action $\mathcal{S} = \mu_0 M_s^2 \int dt \int_\Omega d^3x \mathcal{L} \equiv \mu_0 M_s^2 V \int dt \langle \mathcal{L} \rangle_\Omega$, where V the finite volume of Ω , $\langle \cdot \rangle_\Omega$ denoting spatial averaging, and the normalized Lagrangian density \mathcal{L} is given by [1, 38]

$$\mathcal{L} = \frac{1}{2} \frac{(\mathbf{u}_0 \times \mathbf{m})}{\omega_M} \cdot \partial_t \mathbf{m} - \mathcal{U} - \kappa \mathbf{u}_0 \cdot \mathbf{m}. \quad (1)$$

The first term plays the role of a kinetic energy density, with $\omega_M = |\gamma| \mu_0 M_s$ a natural frequency scale. As for the "potential" energy density [46, 47], we choose for concreteness $\mathcal{U} = \frac{1}{2} h_0 \mathbf{m} \cdot \mathbf{m} + \frac{1}{2} \lambda_{\text{exc}}^2 \nabla \mathbf{m} : \nabla \mathbf{m} - \frac{1}{2} h_a (\mathbf{e}_a \cdot \mathbf{m})^2 + \mathcal{U}_d$, where $h_0 \mathbf{u}_0$ is the equilibrium effective field, λ_{exc} the exchange length, h_a the anisotropy field along the unit vector \mathbf{e}_a , and $\mathcal{U}_d = -\frac{1}{2} (\nabla \phi)^2 + \mathbf{m} \cdot \nabla \phi$ the DDI contribution with ϕ the magnetic scalar potential. The fields h_0, h_a , and $-\nabla \phi$ shall be understood as having been normalized by $\mu_0 M_s$. Finally, $\kappa(\mathbf{x}, t)$ is a Lagrange multiplier. AM is the conserved quantity associated with a rotation symmetry of the Lagrangian. Let δr_J be the infinitesimal rotation by an angle $\delta \theta$, around a certain Oz axis. It admits a natural decomposition $\delta r_J = \delta r_L \circ \delta r_S$. We introduce a global cylindrical coordinate system $(O; r, \theta, z)$ with local unit vector basis $\{\mathbf{e}_r, \mathbf{e}_\theta, \mathbf{e}_z\}$. The action of δr_J on $\mathbf{m}(\mathbf{x})$ is then given by $\delta r_J : \mathbf{m} \rightarrow \mathbf{m} + \delta \mathbf{m}_J$ and $\frac{\delta \mathbf{m}_J}{\delta \theta} \equiv \frac{\delta \mathbf{m}_L}{\delta \theta} + \frac{\delta \mathbf{m}_S}{\delta \theta} = -\partial_\theta \mathbf{m} + \mathbf{e}_z \times \mathbf{m}$. If we assume the Lagrangian to be invariant under $\delta r_J, \delta r_L$ or δr_S , an application of the Noether's theorem [48] yields respectively, as globally conserved quantities, the projections

along Oz of the volume integrated AM, J^z , OAM, L^z , and SAM, S^z , as [1]

$$J^z = L^z + S^z, \quad (2a)$$

$$L^z = -\mathcal{J}_M \int_{\Omega} d^3x (\mathbf{u}_0 \times \mathbf{m}) \cdot \partial_{\theta} \mathbf{m}, \quad (2b)$$

$$S^z = +\mathcal{J}_M \int_{\Omega} d^3x (\mathbf{u}_0 \times \mathbf{m}) \cdot (\mathbf{e}_z \times \mathbf{m}), \quad (2c)$$

in which $\mathcal{J}_M = M_S/(2|\gamma|)$ emerges as a natural scale of AM density for the linear SWs.

We next clarify the relation between the AM densities and azimuthal SW eigenmodes. The Euler-Lagrange equation for \mathbf{m} associated with \mathcal{S} reads $\partial_t \mathbf{m} = \omega_M \mathbf{u}_0 \times \frac{\delta \mathcal{U}}{\delta \mathbf{m}}$, under the constraint $\mathbf{u}_0 \cdot \mathbf{m} = 0$, which we recognize as the linearization of the Landau-Lifshitz equation [49]. The Fourier transform in time $\mathbf{m}(\mathbf{x}, t) = \Re[\tilde{\mathbf{m}}(\mathbf{x})e^{-i\omega t}]$ with $\omega \in \mathbb{R}$ and $\tilde{\mathbf{m}} \in \mathbb{C}^3/\{\mathbf{u}_0 \cdot \tilde{\mathbf{m}} = 0\}$ yields an eigenvalue problem $\omega \tilde{\mathbf{m}} = \hat{\mathcal{O}} \tilde{\mathbf{m}}$, where the integro-differential operator $\hat{\mathcal{O}}$ is derived from \mathcal{U} and \mathbf{u}_0 . The resultant SW eigenmodes, labelled by a stand-in mode index ν to be specified by boundary conditions, satisfy two general properties [45, 50, 51]: (i) if $\{\omega_{\nu}, \tilde{\mathbf{m}}_{\nu}\}$ is a SW eigenpair, then $\{-\omega_{\nu}, \tilde{\mathbf{m}}_{\nu}^*\}$ is one as well, representing the same physical state, and (ii) the SW eigenmodes satisfy the orthogonality relation [45]

$$-\frac{\mathbf{i}}{2} \frac{\langle (\mathbf{u}_0 \times \tilde{\mathbf{m}}_{\nu}^*) \cdot \tilde{\mathbf{m}}_{\nu'} \rangle_{\Omega}}{\text{sgn}(\omega_{\nu})} = A_{\nu}^2 \delta_{\nu, \nu'}, \quad (3)$$

with $A_{\nu} > 0$ being *defined* as the natural norm of the mode. If the action is invariant under δr_J , the eigenmodes can be chosen as eigenfunctions of the associated infinitesimal generator *i.e.*, $\mathbf{m}_{\nu, n_J} = \Re[\tilde{\mathbf{m}}_{\nu, n_J}(r, z)e^{i(n_J\theta - \omega_{\nu, n_J}t)}]$ with $\tilde{\mathbf{m}}_{\nu, n_J} \equiv \tilde{m}_{\nu, n_J}^r(r, z)\mathbf{e}_r + \tilde{m}_{\nu, n_J}^{\theta}(r, z)\mathbf{e}_{\theta} + \tilde{m}_{\nu, n_J}^z(r, z)\mathbf{e}_z$ and $n_J \in \mathbb{Z}$ being an eigenvalue of δr_J , since $[(\mathbf{e}_z \times \cdot) - \partial_{\theta}] \tilde{\mathbf{m}}_{\nu, n_J} = -\mathbf{i}n_J \tilde{\mathbf{m}}_{\nu, n_J}$. Substituting this waveform into Eq. (2a) gives

$$J_{\nu, n_J}^z = \text{sgn}(\omega_{\nu, n_J}) n_J V \mathcal{J}_M A_{\nu, n_J}^2. \quad (4)$$

If the action is additionally invariant under δr_L and δr_S , the eigenmodes can be eigenfunctions of both associated infinitesimal generators *i.e.*, $\mathbf{m}_{\nu, n_L, n_S}^0 = m_{\nu, n_L}^0(r, z) \Re[(\mathbf{e}_r + \mathbf{i}n_S \mathbf{e}_{\theta})e^{i(n_J\theta - n_S\omega_{\nu, n_L}^0 t)}]$, with the corresponding eigenvalues $n_L = n_J - n_S$, $n_L \in \mathbb{Z}$, $n_S = \pm 1$ and $\omega_{\nu, n_L}^0 > 0$; as $\mathbf{e}_z \times (\mathbf{e}_r \pm \mathbf{i}n_S \mathbf{e}_{\theta}) = \mp \mathbf{i}(\mathbf{e}_r \pm \mathbf{i}n_S \mathbf{e}_{\theta})$. Then Eqs. (2b-2c) give $L_{\nu, n_J}^z = n_S n_L V \mathcal{J}_M A_{\nu, n_J}^2$, and $S_{\nu, n_J}^z = V \mathcal{J}_M A_{\nu, n_J}^2$. The canonical quantization for constrained systems [1, 52, 53] establishes $V \mathcal{J}_M A_{\nu, n_J}^2 = \hbar$ for single magnon states, confirming the quantization of conserved angular momenta per magnon.

Let us elaborate on the physical meaning of the angular momentum labels n_J and n_L . The Lagrangian is

generically invariant under δr_J if: (i) the region Ω , (ii) the equilibrium texture \mathbf{u}_0 , and (iii) all the magnetic material properties, are invariant under δr_J . This defines a broad class of axisymmetric ferromagnets, such as YIG spheres [13, 16] or mesoscopic disks in one of their known axisymmetric equilibria [54–57]. According to Eq. (4), n_J is a measure of AM up to the choice $\text{sgn}(\omega_{\nu, n_J}) = \pm 1$. In all concrete calculations, we use the positive sign convention, by which $n_J > 0$ represents positive AM. OAM can be associated to the integer label n_L *only if* the Lagrangian is invariant under δr_L , which occurs if, in addition to (i-iii), we also have: (iv) $\mathbf{u}_0 = \mathbf{e}_a = \mathbf{e}_z$, and (v) a negligible DDI [38, 39], [58]. Hereafter, we further specialize the problem to a sufficiently thin disk so that \mathbf{m} can be considered independent of z . Then, under (i-v), the equation $\omega \mathbf{m} = \hat{\mathcal{O}} \mathbf{m}$ reduces to

$$\omega_{n_R, n_L, n_S}^0 m_{n_R, n_L}^0 = n_S \left[h_0 + \lambda_{\text{exc}}^2 \left(\frac{n_L^2}{r^2} - \nabla_{\perp}^2 \right) \right] m_{n_R, n_L}^0, \quad (5)$$

in which $\nabla_{\perp}^2 \equiv \partial_r^2 + (1/r)\partial_r$ and n_R is the associated radial index. It immediately follows that $\omega_{n_R, n_L, n_S}^0 = n_S \omega_{n_R, |n_L|}^0$ with $\omega_{n_R, |n_L|}^0 > 0$, while the corresponding eigenvector amplitudes can be expressed as $\tilde{\mathbf{m}}_{n_R, n_L, n_S}^0 = m_{n_R, |n_L|}^0(r, z)(\mathbf{e}_r + \mathbf{i}n_S \mathbf{e}_{\theta})$. Similarly to n_J , n_L quantifies OAM only up to the sign of eigenfrequency, or equivalently the eigenvalue n_S of δr_S that carries no physical significance. In Fig. 2a) we show the AM and OAM of the SW eigenstates derived from Eq. (5). The dotted line highlights in red/blue the number of oscillatory cycles $|n_J|$ of the radial component of \mathbf{m} around the disk circumference. It differs by one unit from $|n_L|$, which counts the number of revolutions of \mathbf{m} , encoded in the cyclic color wheel. For $n_L \neq 0$ and fixed n_S , the sign of n_L indicates whether the direction of rotation of the Cartesian component wavefront (large circular arrow) is identical or reversed compared to the direction of local precession (small circular arrow) *i.e.*, whether the OAM is parallel or anti-parallel to the SAM.

We now introduce the general notion of magnon SOI. Consider a system where (i-v) are satisfied and fix $n_L \in \mathbb{Z}$. The magnons come in degenerate pairs $n_J = \pm n_L + n_S$ with identical radial profile and opposite values of the OAM $\propto \pm n_S n_L$. The SOI manifests itself through the lift of this degeneracy, and is quantified by the frequency splittings between magnons with opposite OAM *i.e.*, $\text{SOI}_{n_R, n_L} = (\omega_{n_R, 1+n_L} - \omega_{n_R, 1-n_L})$ under the convention $n_S = +1$. In the present case, the splitting is induced by DDI. When neglecting the DDI, all the SW eigenmodes of the disk are circularly polarized with right-handed precession, due to the time reversal symmetry breaking associated with the equilibrium magnetization as shown in Fig. 2a). However, they induce a dynamic dipolar field with both right- and left-handed circularly polarized components in the disk plane (see Fig. 2b)). More quantitatively, the linear operator $\hat{\mathcal{O}}$ can

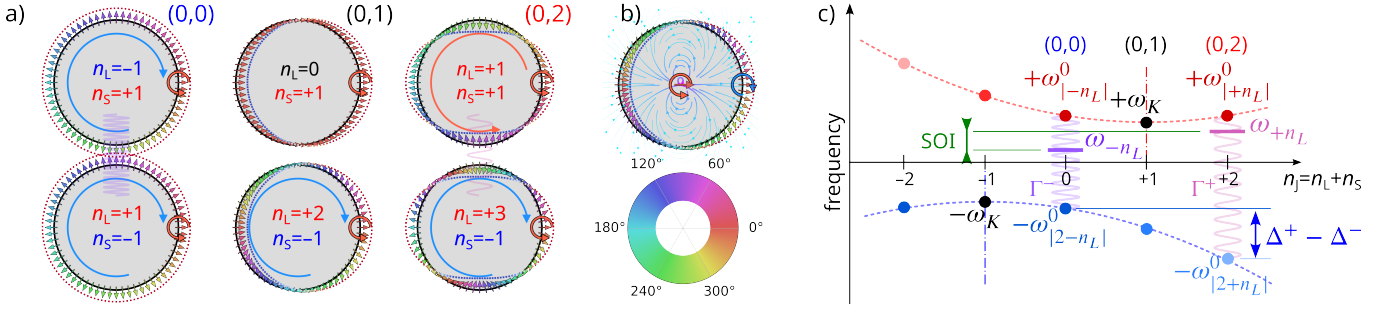


FIG. 2. a) Azimuthal pattern of SW modes $(0, n_J)$ for $H_0 \gg H_{\text{sat}}$. The index $|n_J|$ counts the number of oscillations in the radial component (see dotted line), while $|n_L|$ counts the number of revolutions of \mathbf{m} (see colorwheel repetition). b) Illustration of the DDI produced by a right-handed rotating magnetic dipole at the center. The azimuthal stray magnetic field pattern is a superposition of $n_L = +2, n_S = -1$ and $n_L = 0, n_S = +1$ azimuthal textures. The former component having left-handed local precession provides coupling to modes with $n_S = -1$ sharing the same n_J (wiggly lines). c) Graphical representation of $\hat{O}_d^{(-)}$, in terms of the lowest energy eigenstates of \hat{O}_0 (red and blue dots). The unperturbed $\pm n_L$ eigenstates lower their energy through $\hat{O}_d^{(-)}$ by an amount inversely proportional to the frequency gap $\omega_{|n_L|}^0 + \omega_{|2 \pm n_L|}^0$, forming elliptically precessing states via mixing of $n_S = \pm 1$ subspaces. The SOI splitting is the spectral signature of the rotating nature of the wavefront.

be split as $\hat{O} = \hat{O}_0 + \hat{O}_d^{(+)} + \hat{O}_d^{(-)}$ with \hat{O}_0 corresponding to the equilibrium effective field and exchange contributions. $\hat{O}_d^{(\pm)}$ are defined to be parts of the DDI that commute and anti-commute with δr_S respectively. Therefore, represented in the basis $\{\tilde{\mathbf{m}}_{n_R, n_L, n_S}^0, n_L \in \mathbb{Z}, n_S = \pm 1\}$, $\hat{O}_0 + \hat{O}_d^{(+)}$ leaves the $n_S = \pm 1$ subspaces invariant, while $\hat{O}_d^{(-)}$ swaps the two and is the sole source of SOI, with $\hat{O}_d^{(\pm)} \mathbf{m}_{n_R, n_L, n_S}^0$ proportional to right- and left-handed components of the dynamical stray field. They both conserve $n_J = n_L + n_S$, hence $\hat{O}_d^{(-)}$ uniquely couples n_L with $n_S = +1$ to $n_L + 2$ with $n_S = -1$, breaking the $\pm n_L$ spectral symmetry as illustrated in Fig. 2c) where the eigenvalues ω_{n_R, n_L, n_S}^0 of \hat{O}_0 *i.e.*, “unperturbed” frequency spectrum, are plotted for the $n_R = 0$ branch with the dotted lines being a guide for the eyes. In some intermediate field range $h_0 \gtrsim 1$, we can try to obtain a semi-quantitative insight into the emergence of the SOI by considering the DDI as a perturbation. Focusing on the $n_R = 0$ branch, and up to second order in the DDI, we obtain [1]

$$\text{SOI}_{0, n_L} = \sum_{n_R} \left[\frac{\Gamma_{\langle 0|n_R\rangle, n_L}^-}{2\omega_K + \Delta_{\langle 0|n_R\rangle, n_L}^-} - \frac{\Gamma_{\langle 0|n_R\rangle, n_L}^+}{2\omega_K + \Delta_{\langle 0|n_R\rangle, n_L}^+} \right], \quad (6)$$

where $\Gamma_{\langle 0|n_R\rangle, n_L}^{\pm} = \langle m_{n_R, |2 \pm n_L|}^0 \hat{O}_d^{(\pm)} m_{0, |n_L|}^0 \rangle_{\Omega}$ and $\Delta_{\langle 0|n_R\rangle, n_L}^{\pm} = \omega_{0, |n_L|}^0 + \omega_{n_R, |2 \pm n_L|}^0 - 2\omega_K$ with ω_K being the frequency of the quasi-uniform Kittel mode for the disk. By direct inspection of Eq.(6) we obtain the confirmation of a field-controllable SOI, with a leading asymptotic term inversely proportional to ω_K . The splitting between $n_L = \pm 1, n_S = +1$ through the hybridization with $n_L = 2 \pm 1, n_S = -1$ is illustrated in Fig. 2c). The eigenfrequencies and eigenmodes of \hat{O}_0 can be obtained semi-analytically from a Galerkin projection of the corresponding spectral boundary value problem over a trun-

cated basis of the analytical exchange SWs, while explicit integral forms of the matrix elements of \hat{O}_d^{\pm} on the same basis can be obtained [1]. This in principle enables a numerical evaluation of the approximate SOI frequency split Eq. (6). However, it is found more straightforward, and more accurate over the whole field range, to perform a Galerkin projection of the full spectral boundary value problem associated with \hat{O} [1]. The SOI frequency split can then be directly obtained from the numerically estimated exchange-dipole SW frequencies. This is the method that has been used to generate the continuous line in Fig. 1d).

We now compare the semi-analytical prediction with the experiment. In Fig. 1d), we plot the variation of the experimentally determined SOI splitting as a function of the magnetic field strength H_0 identified with $\mu_0 M_s h_0$. The superimposed solid line is the theoretically computed $\text{SOI}_{0,1}$. We see quantitative agreement when the field strength is above $\mu_0 M_s = 0.17$ T. As H_{sat} is approached from above, however, a significant deviation appears. We also observe that the experimental value of H_{sat} in Fig. 1 is significantly lower than the semi-analytical prediction. We attribute these to a slight misalignment of the field with respect to the normal of the disk. To account for this, we have performed a full 3D micromagnetic simulation of the splitting between the ν_0 and ν_2 modes as a function of the applied magnetic field, assuming first perfect alignment with the normal and then a 0.7° misalignment. When the field is perfectly aligned, the simulation reproduces exactly the semi-analytical results [1]. For the misaligned case, the numerical result is shown as a dashed line in Fig. 1d). We now obtain full agreement with the simulation in the full range of magnetic fields explored experimentally.

In summary, we provide here a comprehensive semi-analytical picture for identifying the pseudo-OAM of azimuthal spin-waves and we show a practical implementa-

tion. The method relies on the fact in magnetic systems the SOI is controllable by the magnetic field and can be made very large. Future direction is to transfer this SOI to other vector fields such as photons or phonons by hybridization opening a new avenue to identify the OAM.

We sincerely thank Prof. Y. Otani from the University of Tokyo and Prof. C. Serpico from the University Federico II of Naples for their invaluable insights and thought-provoking discussions. This work was partially supported by the EU-project HORIZON-EIC-2021-PATHFINDER OPEN PALANTIRI-101046630; the French Grants ANR-21-CE24-0031 Harmony; the PEPR SPIN - MAGISTRAL ANR-24-EXSP-0004; the French Renatech network; and the REIMEI Research Program of Japan Atomic Energy Agency. K.Y. acknowledges support from JST PRESTO Grant No. JPMHPR20LB, Japan, JSPS KAKENHI (No. 21K13886), and JSPS Bilateral Program Number JPJSBP120245708.

* Corresponding author : tvalet@mphysx.com

† Corresponding author : oklein@cea.fr

- [1] T. Valet, K. Yamamoto, B. Pigeau, G. de Loubens, and O. Klein, Field theory of linear spin-waves in finite textured ferromagnets (2025), 2503.06557 [cond-mat.mesh-hall].
- [2] R. Chen, H. Zhou, M. Moretti, X. Wang, and J. Li, Orbital angular momentum waves: Generation, detection, and emerging applications, *IEEE Communications Surveys & Tutorials* **22**, 840 (2020).
- [3] S. Franke-Arnold, 30 years of orbital angular momentum of light, *Nat. Rev. Phys.* **4**, 361 (2022).
- [4] P. Couillet, L. Gil, and F. Rocca, Optical vortices, *Optics Communications* **73**, 403 (1989).
- [5] L. Allen, M. W. Beijersbergen, R. J. C. Spreeuw, and J. P. Woerdman, Orbital angular momentum of light and the transformation of laguerre-gaussian laser modes, *Phys. Rev. A* **45**, 8185 (1992).
- [6] S. W. Hancock, S. Zahedpour, and H. M. Milchberg, Mode structure and orbital angular momentum of spatiotemporal optical vortex pulses, *Phys. Rev. Lett.* **127**, 193901 (2021).
- [7] K. Y. Bliokh and Y. P. Bliokh, Momentum, angular momentum, and spin of waves in an isotropic collisionless plasma, *Phys. Rev. E* **105**, 065208 (2022).
- [8] W. L. Jones, Asymmetric wave-stress tensors and wave spin, *Journal of Fluid Mechanics* **58**, 737747 (1973).
- [9] J.-L. Thomas and R. Marchiano, Pseudo angular momentum and topological charge conservation for nonlinear acoustical vortices, *Phys. Rev. Lett.* **91**, 244302 (2003).
- [10] D. A. Garanin and E. M. Chudnovsky, Angular momentum in spin-phonon processes, *Phys. Rev. B* **92**, 024421 (2015).
- [11] M. E. McIntyre, On the wave momentum myth, *Journal of Fluid Mechanics* **106**, 331347 (1981).
- [12] S. Streib, Difference between angular momentum and pseudoangular momentum, *Phys. Rev. B* **103**, L100409 (2021).
- [13] A. Osada, R. Hisatomi, A. Noguchi, Y. Tabuchi, R. Yamazaki, K. Usami, M. Sadgrove, R. Yalla, M. Nomura, and Y. Nakamura, Cavity optomagnonics with spin-orbit coupled photons, *Phys. Rev. Lett.* **116**, 223601 (2016).
- [14] J. A. Haigh, A. Nunnenkamp, A. J. Ramsay, and A. J. Ferguson, Triple-resonant brillouin light scattering in magneto-optical cavities, *Phys. Rev. Lett.* **117**, 133602 (2016).
- [15] X. Zhang, N. Zhu, C.-L. Zou, and H. X. Tang, Optomagnonic whispering gallery microresonators, *Phys. Rev. Lett.* **117**, 123605 (2016), see also Erratum: *Phys. Rev. Lett.* **121**, 199901 (2018).
- [16] S. Sharma, Y. M. Blanter, and G. E. W. Bauer, Light scattering by magnons in whispering gallery mode cavities, *Phys. Rev. B* **96**, 094412 (2017).
- [17] A. Osada, A. Gloppe, Y. Nakamura, and K. Usami, Orbital angular momentum conservation in brillouin light scattering within a ferromagnetic sphere, *New Journal of Physics* **20**, 103018 (2018).
- [18] A. Gloppe, R. Hisatomi, Y. Nakata, Y. Nakamura, and K. Usami, Resonant magnetic induction tomography of a magnetized sphere, *Physical Review Applied* **12**, 014061 (2019).
- [19] K. An, A. N. Litvinenko, R. Kohno, A. A. Fuad, V. V. Naletov, L. Vila, U. Ebels, G. de Loubens, H. Hurd-equent, N. Beaulieu, J. Ben Youssef, N. Vukadinovic, G. E. W. Bauer, A. N. Slavin, V. S. Tiberkevich, and O. Klein, Coherent long-range transfer of angular momentum between magnon kittel modes by phonons, *Phys. Rev. B* **101**, 060407 (2020).
- [20] M. Xu, K. Yamamoto, J. Puebla, K. Baumgaertl, B. Rana, K. Miura, H. Takahashi, D. Grundler, S. Maekawa, and Y. Otani, Nonreciprocal surface acoustic wave propagation via magneto-rotation coupling, *Science Advances* **6**, eabb1724 (2020).
- [21] R. Sasaki, Y. Nii, and Y. Onose, Magnetization control by angular momentum transfer from surface acoustic wave to ferromagnetic spin moments, *Nat. Commun.* **12**, 2599 (2021).
- [22] R. Schlitz, L. Siegl, T. Sato, W. Yu, G. E. W. Bauer, H. Huebl, and S. T. B. Goennenwein, Magnetization dynamics affected by phonon pumping, *Physical Review B* **106**, 10.1103/physrevb.106.014407 (2022).
- [23] K. An, C. Kim, K.-W. Moon, R. Kohno, G. Olivetti, G. de Loubens, N. Vukadinovic, J. Ben Youssef, C. Hwang, and O. Klein, Optimizing the magnon-phonon cooperativity in planar geometries, *Phys. Rev. Appl.* **20**, 014046 (2023).
- [24] L. Liao, J. Puebla, K. Yamamoto, J. Kim, S. Maekawa, Y. Hwang, Y. Ba, and Y. Otani, Valley-selective phonon-magnon scattering in magnetoelastic superlattices, *Physical Review Letters* **131**, 10.1103/physrevlett.131.176701 (2023).
- [25] J. Leach, M. J. Padgett, S. M. Barnett, S. Franke-Arnold, and J. Courtial, Measuring the orbital angular momentum of a single photon, *Phys. Rev. Lett.* **88**, 257901 (2002).
- [26] M. Buess, R. Höllinger, T. Haug, K. Perzlmaier, U. Krey, D. Pescia, M. R. Scheinfein, D. Weiss, and C. H. Back, Fourier transform imaging of spin vortex eigenmodes, *Physical Review Letters* **93**, 10.1103/physrevlett.93.077207 (2004).
- [27] J. P. Park and P. A. Crowell, Interactions of spin waves with a magnetic vortex, *Physical Review Letters* **95**, 167201 (2005).

- [28] K. Vogt, O. Sukhostavets, H. Schultheiss, B. Obry, P. Pirro, A. A. Serga, T. Sebastian, J. Gonzalez, K. Y. Guslienko, and B. Hillebrands, Optical detection of vortex spin-wave eigenmodes in microstructured ferromagnetic disks, *Physical Review B* **84**, 174401 (2011).
- [29] K. Schultheiss, R. Verba, F. Wehrmann, K. Wagner, L. Krber, T. Hula, T. Hache, A. Kákay, A. Awad, V. Tiberkevich, A. Slavin, J. Fassbender, and H. Schultheiss, Excitation of whispering gallery magnons in a magnetic vortex, *Physical Review Letters* **122**, 10.1103/physrevlett.122.097202 (2019).
- [30] B. A. Ivanov, H. J. Schnitzer, F. G. Mertens, and G. M. Wysin, Magnon modes and magnon-vortex scattering in two-dimensional easy-plane ferromagnets, *Physical Review B* **58**, 84648474 (1998).
- [31] M. Buess, T. P. J. Knowles, R. Höllinger, T. Haug, U. Krey, D. Weiss, D. Pescia, M. R. Scheinfein, and C. H. Back, Excitations with negative dispersion in a spin vortex, *Physical Review B* **71**, 10.1103/physrevb.71.104415 (2005).
- [32] K. Y. Guslienko, A. N. Slavin, V. Tiberkevich, and S.-K. Kim, Dynamic origin of azimuthal modes splitting in vortex-state magnetic dots, *Physical Review Letters* **101**, 10.1103/physrevlett.101.247203 (2008).
- [33] R. Verba, L. Körber, K. Schultheiss, H. Schultheiss, V. Tiberkevich, and A. Slavin, Theory of three-magnon interaction in a vortex-state magnetic nanodot, *Physical Review B* **103**, 10.1103/physrevb.103.014413 (2021).
- [34] J. Rychlý, V. S. Tkachenko, J. W. Klos, A. Kuchko, and M. Krawczyk, Spin wave modes in a cylindrical nanowire in crossover dipolar-exchange regime, *Journal of Physics D: Applied Physics* **52**, 075003 (2018).
- [35] C. Jia, D. Ma, A. Schäfer, and J. Berakdar, Twisted magnon beams carrying orbital angular momentums, *Nature Comm.* **10**, 2077 (2019).
- [36] Y. Jiang, H. Y. Yuan, Z.-X. Li, Z. Wang, H. W. Zhang, Y. Cao, and P. Yan, Twisted magnon as a magnetic tweezer, *Phys. Rev. Lett.* **124**, 217204 (2020).
- [37] S. Lee and S. K. Kim, Generation of magnon orbital angular momentum by a skyrmion-textured domain wall in a ferromagnetic nanotube, *Frontiers in Physics* **10**, 10.3389/fphy.2022.858614 (2022).
- [38] V. Tsukernik, Some features of the gyromagnetic effect in ferroelectrics at low temperatures, *JETP* **23**, 1085 (1966), [*Zh. Eksp. Teor. Fiz.*, **50**(6), 1631 (1966)].
- [39] E. Goldshtein and V. Tsukernik, Angular momentum of a heisenberg ferromagnet with a magnetic dipole interaction, *JETP* **60**, 764 (1984), [*Zh. Eksp. Teor. Fiz.*, **87**, 1330 (1984)].
- [40] P. Yan, A. Kamra, Y. Cao, and G. E. W. Bauer, Angular and linear momentum of excited ferromagnets, *Phys. Rev. B* **88**, 144413 (2013).
- [41] O. Tchernyshyov, Conserved momenta of a ferromagnetic soliton, *Annals of Physics* **363**, 98 (2015).
- [42] R. R. Neumann, A. Mook, J. Henk, and I. Mertig, Orbital magnetic moment of magnons, *Phys. Rev. Lett.* **125**, 117209 (2020).
- [43] R. S. Fishman, J. S. Gardner, and S. Okamoto, Orbital angular momentum of magnons in collinear magnets, *Phys. Rev. Lett.* **129**, 167202 (2022), see also Erratum: *Phys. Rev. Lett.* **130**, 059901 (2023).
- [44] J. Liu, L. Wang, and K. Shen, Spin-orbit coupling and linear crossings of dipolar magnons in van der waals antiferromagnets, *Phys. Rev. B* **102**, 144416 (2020).
- [45] V. V. Naletov, G. de Loubens, G. Albuquerque, S. Borlenghi, V. Cros, G. Faini, J. Grollier, H. Hurdequint, N. Locatelli, B. Pigeau, A. N. Slavin, V. S. Tiberkevich, C. Ulysse, T. Valet, and O. Klein, Identification and selection rules of the spin-wave eigenmodes in a normally magnetized nanopillar, *Phys. Rev. B* **84**, 224423 (2011).
- [46] W. Brown, *Micromagnetics* (Interscience, 1963).
- [47] J. Miltat, G. Albuquerque, and A. Thiaville, An introduction to micromagnetics in the dynamic regime, in *Spin Dynamics in Confined Magnetic Structures I*, edited by B. Hillebrands and K. Ounadjela (Springer Berlin Heidelberg, Berlin, Heidelberg, 2002) pp. 1–33.
- [48] S. Weinberg, *The Quantum Theory of Fields, Volume 1: Foundations* (Cambridge University Press, 1995).
- [49] L. D. Landau and E. Lifshitz, On the theory of the dispersion of magnetic permeability in ferromagnetic bodies, *Phys. Z. Sowjet.* **8**, 153 (1935).
- [50] D. Mills, Quantum theory of spin waves in finite samples, *Journal of Magnetism and Magnetic Materials* **306**, 16 (2006).
- [51] M. dAquinio, C. Serpico, G. Miano, and C. Forestiere, A novel formulation for the numerical computation of magnetization modes in complex micromagnetic systems, *Journal of Computational Physics* **228**, 6130 (2009).
- [52] P. A. M. Dirac, Generalized hamiltonian dynamics, *Canadian Journal of Mathematics* **2**, 129148 (1950).
- [53] P. A. M. Dirac, *Lectures on quantum mechanics*, *Dover ed.*, Dover Books On Physics (Dover Publications, 2003).
- [54] K. Y. Guslienko, Magnetic vortex state stability, reversal and dynamics in restricted geometries, *Journal of Nanoscience and Nanotechnology* **8**, 2745 (2008).
- [55] B. Taurel, T. Valet, V. V. Naletov, N. Vukadinovic, G. de Loubens, and O. Klein, Complete mapping of the spin-wave spectrum in a vortex-state nanodisk, *Phys. Rev. B* **93**, 184427 (2016).
- [56] N. Vukadinovic and F. Boust, Spin-wave excitations of domain walls in bubble-state magnetic nanoelements, *Phys. Rev. B* **84**, 224425 (2011).
- [57] S. Rohart and A. Thiaville, Skyrmion confinement in ultrathin film nanostructures in the presence of dzyaloshinskii-moriya interaction, *Phys. Rev. B* **88**, 184422 (2013).
- [58] It shall be noted that a negligible DDI is a *sufficient* condition for magnons to carry separately conserved and quantized SAM and OAM, but *not* a necessary condition.